






Nickel(II), copper(II), cobalt(II), and palladium(II) complexes with a Schiff base: crystal structure, DFT study and copper complex catalyzed aerobic oxidation of alcohol to aldehyde

Kuladip Sarma, Namita Devi, Mukul Kalita, Bipul Sarma & Pranjit Barman


To cite this article: Kuladip Sarma, Namita Devi, Mukul Kalita, Bipul Sarma & Pranjit Barman (2015) Nickel(II), copper(II), cobalt(II), and palladium(II) complexes with a Schiff base: crystal structure, DFT study and copper complex catalyzed aerobic oxidation of alcohol to aldehyde, Journal of Coordination Chemistry, 68:20, 3685-3700, DOI: [10.1080/00958972.2015.1075241](https://doi.org/10.1080/00958972.2015.1075241)

To link to this article: <http://dx.doi.org/10.1080/00958972.2015.1075241>

 View supplementary material 

 Accepted author version posted online: 29 Jul 2015.
Published online: 20 Aug 2015.

 Submit your article to this journal 

 Article views: 170

 View related articles 

 View Crossmark data 

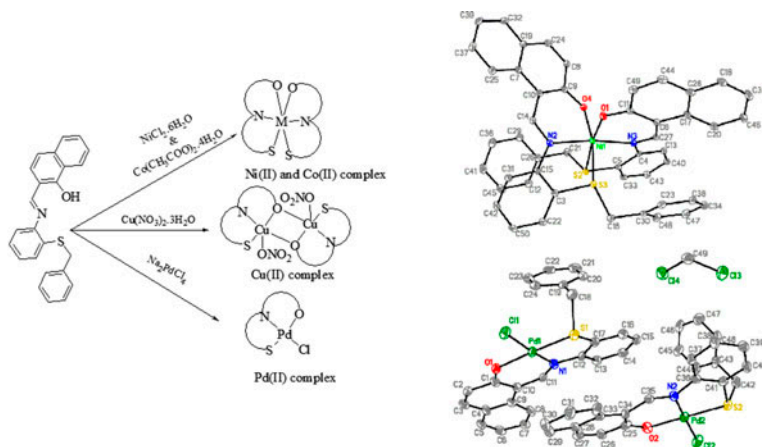
Nickel(II), copper(II), cobalt(II), and palladium(II) complexes with a Schiff base: crystal structure, DFT study and copper complex catalyzed aerobic oxidation of alcohol to aldehyde

KULADIP SARMA[†], NAMITA DEVI[†], MUKUL KALITA[†], BIPUL SARMA[‡] and PRANJIT BARMAN^{*†}

[†]Department of Chemistry, National Institute of Technology, Silchar, India

[‡]Department of Chemical Sciences, Tezpur University, Tezpur, India

(Received 3 January 2015; accepted 3 July 2015)



Ni(II), Cu(II), Co(II), and Pd(II) complexes were synthesized with a Schiff base containing thioether with ONS donors chelating to the metal center. The ligand and complexes were characterized by elemental analysis, FT-IR, ¹H-NMR, UV–visible spectroscopy and magnetic studies. The crystal structures of the ligand and its Ni(II) and Pd(II) complexes were determined by single-crystal X-ray diffraction analysis. Structures revealed that the ligand chelated with Ni(II) and Pd(II) center in slightly distorted octahedral and slightly distorted square planar fashion, respectively. DFT studies of the Pd(II) complex revealed that the calculated structural parameters are very close with the experimentally observed data. The Cu(II) complex shows very good catalytic activity toward the conversion of alcohol to aldehyde under aerobic oxidation with ammonium persulfate.

Keywords: Schiff base; Crystal structure; Catalytic activities; DFT study

*Corresponding author. Email: pranjit@che.nits.ac.in

1. Introduction

Schiff bases have influenced coordination chemistry [1] because they have good coordinating ability to form stable complexes with most transition metal ions. Such behavior of Schiff base offered opportunities for inducing substrate chirality, tuning metal-centered electronic factors, and enhancing the stability of either homogeneous or heterogeneous catalyst [2–11]. Schiff base metal complexes with nitrogen–sulfur donors are important because they mimic biologically significant metalloenzymes [12]. Also, Schiff bases form charge-transfer complexes with O and N with the aid of metals like Ni, Cu, and Co showing the importance as enzyme models. The rapid development of these types of ligands has enhanced the research activity in coordination chemistry. Metal complexes with ONS donors show antitumor, fungicidal, bactericidal, antibacterial, antifungal, anti-inflammatory, and antiviral activities [13–22]. Ni(II) Schiff base complexes efficiently catalyze C–S cross-coupling of thiols with organic chlorides [23]. Ni(II) complexes of chelating ligands incorporating thioether and imine donors have relevant properties with various metalloproteins such as blue copper proteins, hemocyanin, tyrosinase, and metalloenzymes as well as their stability [24–26]. Pd(II) complexes with ONS-donor Schiff bases also have wide catalytic activity in organic transformations such as polymerization of ethylene, epoxidation, allylic alkylation, Heck reaction, and Suzuki–Miyaura coupling reactions [27–31]. Moreover, Cu(II) Schiff base complexes are used as versatile catalysts in various oxygenation reactions in homogeneous as well as heterogeneous conditions [32].

The oxidation of alcohol to aldehyde is an important reaction in organic chemistry. Numerous reagents and methods are reported for these conversions [33–47], but the development of environmentally benign processes is a challenge. Cu(II) complexes are useful metal-mediated catalysts in these conversions.

Here, we synthesize a Schiff base from 2-hydroxynaphthaldehyde and 2-(benzylthio)aniline and a series of metal complexes with Cu(II), Ni(II), Co(II), and Pd(II) ions. We have also studied the catalytic activity of the Cu(II) complex toward aerobic oxidation of alcohol to aldehyde in acetonitrile using ammonium persulfate as oxidant.

2. Experimental

2.1. Materials

All chemicals were used without purification. Nickel chloride hexahydrate, copper nitrate trihydrate, and cobalt acetate tetrahydrate were purchased from Merck India and 2-hydroxynaphthaldehyde and sodium tetrachloropalladate were purchased from Alfa Aesar. All alcohols were purchased from Aldrich. 2-(Benzylthio)aniline was prepared according to the literature method [48]. Solvents used were extra pure grade purchased from Merck India and were dried by the reported procedure [49].

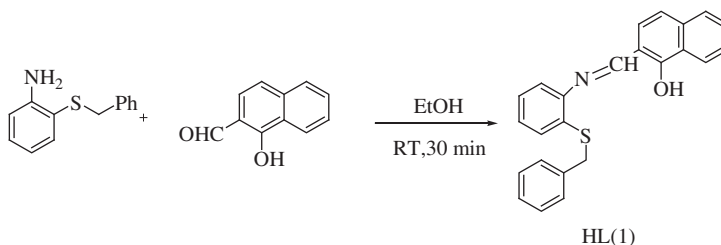
2.2. Methods

Infrared spectra of the ligand and complexes were recorded with a FT-IR-3000 Hyperion Microscope (Bruker, Germany). Elemental analyses were performed on a Flash 2000 Thermo Scientific instrument. $^1\text{H-NMR}$ spectra of the ligand and Pd(II) complex were performed on a VARIAN Mercury plus 300 MHz NMR spectrometer using CDCl_3 as solvent.

Electrical conductivities were measured on a CM-180 Conductivity meter (Elico India). Electronic spectra of the compounds were carried out with a Cary 100 Bio UV–visible spectrometer in DMF. Magnetic susceptibilities were measured on a conventional Gouy balance using freshly prepared $\text{Hg}[\text{Co}(\text{NCS})_4]$ as calibrant using a Magway MSB MK1 Magnetic susceptibility balance, Sherwood Scientific, Cambridge, UK. Melting points were recorded on a Veego melting point apparatus and were uncorrected.

2.3. Synthesis of ligand HL (1)

2-(Benzylthio)aniline (0.215 g, 1 mmol) was dissolved in ethanol. To the above solution, an ethanolic solution of 2-hydroxynaphthaldehyde (0.172 g, 1 mmol) was added dropwise with continuous stirring. The resulting solution was allowed to stir for 30 min at room temperature. The color of the solution changed to dark yellow. The solution was kept at 0 °C for 4 h; a yellow crystalline product formed, was filtered off, washed with 25% ethanol–water, and dried in vacuum (10^{-2} torr). The product was recrystallized in ethanol, giving suitable crystals for single crystal X-ray diffraction analysis. Yield was almost quantitative. m.p.: 185 °C. IR (KBr, cm^{-1}) 3435 (m), 1610 (s), 1457 (s), 1167 (s), 743 (s). $^1\text{H-NMR}$ (CDCl_3 , 300 MHz): δ 15.30 (1H, s, OH), 9.2 (1H, s, CH=N), 7.1–8.09 (12H, m, Ar–H), 4.1 (2H, s, CH_2). UV–vis



Scheme 1. Synthesis of HL (1).

[DMF, λ_{max} , nm (ϵ_{max} , $\text{M}^{-1} \text{cm}^{-1}$): 267 (15,600), 319 (9490), 392 (11,250), 466 (4020). Anal. Calcd for $\text{C}_{24}\text{H}_{19}\text{NOS}$: C, 78.02; H, 5.18; N, 3.79; S, 8.68; O, 4.33. Found: C, 77.95; H, 5.31; N, 3.82; S, 8.54; O, 4.90 (scheme 1).

2.4. Synthesis of complexes

2.4.1. Synthesis of $[\text{NiL}_2]$ (2). HL (1) (0.738 g, 2 mmol) was dissolved in hot methanol followed by the addition of a methanolic solution of NaOH (0.08 g, 2 mmol). A hot methanolic solution of $\text{NiCl}_2 \cdot 6\text{H}_2\text{O}$ (0.237 g, 1 mmol) was added drop-by-drop to the above solution with continuous stirring. The reaction mixture was stirred for 1 h and color of the solution changed to dark brown. Concentrating to half volume and storing for 3–4 days at room temperature gave a dark brown needle-type crystal suitable for single-crystal X-ray diffraction analysis. The crystals were washed several times with 25% methanol–water to remove impurities and dried under vacuum at 10^{-2} torr (Purity was checked by TLC). Yield 65%; m.p.: >300 °C. IR (KBr, cm^{-1}): 1604 (s), 1455 (s), 1167 (s), 750 (s). UV–vis [DMF, λ_{max} , nm (ϵ_{max} , $\text{M}^{-1} \text{cm}^{-1}$): 281 (20,450), 331 (18,050), 496 (15,000), 601 (160). Conductivity (λ_{M} , $\text{S cm}^2 \text{mol}^{-1}$): 18.3. Anal. Calcd for $\text{C}_{48}\text{H}_{36}\text{N}_2\text{O}_2\text{S}_2\text{Ni}$: C, 72.46; H, 4.56; N, 3.52; S, 8.06; O, 4.02. Found: C, 71.89; H, 4.10; N, 3.88; S, 7.87; O, 3.95.

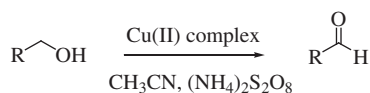
2.4.2. Synthesis of [Cu₂L₂(NO₃)₂] (3). Complex **3** was prepared by the same procedure as **2** with **HL** (**1**) (0.369 g, 1 mmol), NaOH (0.04 g, 1 mmol), and Cu(NO₃)₂·3H₂O (0.199 g, 1 mmol). The color of the solution changed to dark-green and was kept for two days. A green precipitate was collected, washed with 25% methanol–water, and dried under vacuum at 10⁻² torr (Purity was checked by TLC). Yield 62%; m.p.: >300 °C. IR (KBr, cm⁻¹): 1604 (s), 1440 (s), 1297 (s), 1150 (s), 741 (s). UV–vis [DMF, λ_{max}, nm (ε_{max}, M⁻¹ cm⁻¹): 275 (19,650), 320 (17,250), 413 (11,300), 652 (120). Conductivity (λ_M, Scm² mol⁻¹): 21.7. Anal. Calcd for C₄₈H₃₆N₄O₈S₂Cu₂: C, 58.35; H, 3.67; N, 5.67; S, 6.49; O, 12.95. Found: C, 57.79; H, 4.11; N, 5.43; S, 6.21; O, 12.58.

2.4.3. Synthesis of [CoL₂] (4). Complex **4** was prepared by the same procedure as **2** with Co(CH₃COO)₂·4H₂O (0.249 g, 1 mmol). The color of the solution changed to red and was kept for two days. A black precipitate was collected, washed with 25% methanol–water, and dried at 10⁻² torr (Purity was checked by TLC). Yield 70%; m.p.: >300 °C. IR (KBr, cm⁻¹): 1603 (s), 1455 (s), 1170 (s), 749 (s). UV–vis [DMF, λ_{max}, nm (ε_{max}, M⁻¹ cm⁻¹): 281 (13,400), 322 (5625), 485 (2410), 624 (500). Conductivity (λ_M, S cm² mol⁻¹): 26. Anal. Calcd for C₄₈H₃₆N₂O₂S₂Co: C, 72.44; H, 4.56; N, 3.52; S, 8.06; O, 4.02. Found: C, 72.80; H, 4.98; N, 2.77; S, 7.12; O, 4.55.

2.4.4. Synthesis of [PdLCl]·0.5(CH₂Cl₂) (5). An ethanolic solution of Na₂PdCl₄ (0.147 g, 0.5 mmol) was added dropwise to an ethanolic solution of **HL** (**1**) (0.185 g, 0.5 mmol). The resulting solution was stirred under reflux for 1 h. The orange precipitate formed was filtered off and washed with 25% ethanol–water solution several times to remove impurities and dried under vacuum (10⁻² torr) (Purity was checked by TLC). Orange-red, needle-like crystals suitable for single crystal X-ray diffraction analysis were obtained by recrystallization from DCM–hexane (10 : 1) followed by slow evaporation of the solvent (2 days). Yield 68%; m.p.: >300 °C. IR (KBr, cm⁻¹): 1604 (s), 1459 (s), 1170 (s), 746 (s). ¹H-NMR (CDCl₃, 300 MHz): δ 8.95 (1H, s, CH=N), 7.10–7.75 (13 H, m, Ar–H), 4.53 and 4.34 (2H, dd, CH₂). UV–vis [DMF, λ_{max}, nm (ε_{max}, M⁻¹ cm⁻¹): 268 (7965), 347 (3000), 356 (3100), 444 (2575), 472 (2500). Conductivity (λ_M, S cm² mol⁻¹): 24.1. Anal. Calcd for [C₂₄H₁₈NOSPdCl]·0.5(CH₂Cl₂): C, 53.23; H, 3.46; N, 2.53; S, 5.80; O, 2.89. Found: C, 53.39; H, 3.40; N, 2.45; S, 5.64; O, 2.74.

2.5. General procedure for Cu(II) complex catalyzed aerobic oxidation of alcohol to aldehyde

Here, we have reported aerobic oxidation of alcohol to aldehyde using **3**. In this method, substrate (4 mmol), 5 mol% Cu(II) complex, and ammonium persulfate (5 mmol) were added to 20 mL acetonitrile. The reaction mixture was stirred at room temperature. The conversion takes place within 2 min, and the progress of the reaction was monitored by TLC. The product was extracted with EtOAc and purified by column chromatography. The reaction scheme is shown in scheme 2.



Scheme 2. Oxidation of alcohol to aldehyde.

Table 1. Crystal structure and structure refinement details for **1**, **2**, and **5**.

Compound	1	2	5
CCDC entry no.	997116	997117	997118
Empirical formula	C ₂₄ H ₁₉ NOS	C ₄₈ H ₃₆ N ₂ NiO ₂ S ₂	C ₄₉ H ₃₈ Cl ₄ N ₂ O ₂ Pd ₂ S ₂
Formula weight	369.46	795.62	1105.53
<i>T</i> (K)	298(2)	100(2)	296(2)
λ (Å)	0.71073	0.71073	0.71073
Crystal system	Tetragonal	Triclinic	Monoclinic
Space group	P4(1)	P-1	P2(1)/c
Unit cell dimensions			
<i>a</i> (Å)	18.2731(8)	11.1974(5)	11.2548(7)
<i>b</i> (Å)	18.2731(8)	13.4777(5)	20.4902(14)
<i>c</i> (Å)	5.3436(3)	14.4106(6)	19.2916(11)
α (°)	90.00	96.868(3)	90.00
β (°)	90.00	110.113(4)	93.710(5)
γ (°)	90.00	110.134(4)	90.00
<i>V</i> (Å ³)	1784.25(15)	1846.20(12)	4439.6(5)
<i>Z</i>	4	2	4
<i>D</i> _{calc} (Mg m ⁻³)	1.375	1.431	1.654
μ (mm ⁻¹)	1.708	2.166	9.972
<i>F</i> (0 0 0)	776	828	2216
Crystal size (mm ³)	0.35 × 0.17 × 0.12	0.27 × 0.21 × 0.11	0.21 × 0.14 × 0.08
θ (°)	3.42–66.53	3.63–66.60	3.94–66.60
Index ranges	–21 ≤ <i>h</i> ≤ 19 –21 ≤ <i>k</i> ≤ 17 –6 ≤ <i>l</i> ≤ 4	–13 ≤ <i>h</i> ≤ 11 –12 ≤ <i>k</i> ≤ 16 –16 ≤ <i>l</i> ≤ 17	–12 ≤ <i>h</i> ≤ 13 –24 ≤ <i>k</i> ≤ 16 –22 ≤ <i>l</i> ≤ 16
Reflections collected	4072	10,570	13,789
Independent reflections (<i>R</i> _{int})	2153(0.0547)	6445(0.0297)	7305(0.0957)
Completeness (%)	1.22/0.68	99.00	93.20
Absorption correction	Multi-scan (SADABS)	Multi-scan (SADABS)	Multi-scan (SADABS)
Max and min transmission	0.8213 and 0.5863	0.7966 and 0.5924	0.5026 and 0.2286
Refinement method	Full matrix least-squares on <i>F</i> ²	Full matrix least-squares on <i>F</i> ²	Full matrix least-squares on <i>F</i> ²
Data/restraints/parameters	2153/1/249	6445/0/640	7305/0/550
Goodness-of-fit on <i>F</i> ²	1.007	1.066	1.035
Final <i>R</i> indices [<i>I</i> > 2σ(<i>I</i>)]	R1 = 0.0488, wR2 = 0.1055	R1 = 0.0352, wR2 = 0.1031	R1 = 0.0975, wR2 = 0.2280
Largest diff. in peak/hole (e Å ⁻³)	0.241/–0.254	0.375/–0.394	2.102/–0.972

2.6. Crystallography

All data were collected on a Bruker APEX-II CCD diffractometer with graphite-monochromated Cu K α radiation by the ω -scan technique at 298 K (**1**), 100 K (**2**), and 296 K (**5**). Structures were determined using SHELXS-97 [50, 51]. Cell measurement and data reduction were done by Bruker SAINT [52]. Multi-scan method (SADABS) was used for absorption corrections [52]. Full-matrix least-squares on *F*² were performed using the SHELXS-97 program. All non-H atoms were refined in anisotropic approximation using reflections with *I* > 2σ(*I*). Crystal data and structure refinements of **1**, **2**, and **5** are given in table 1.

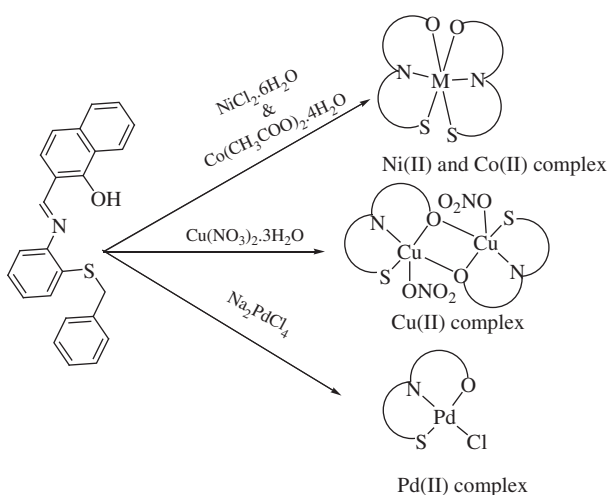
2.7. DFT calculation

Full geometry optimization of Pd(II) complex was performed using Gaussian 09W [53]. Structural calculation was carried out using B3LYP method and mixed basis sets of LanL2DZ for Pd and 6-31+G(d) for all other atoms, i.e., Cl, S, N, O, C, and H.

3. Results and discussion

3.1. Synthesis

The reactions of ONS-donor Schiff base ligand with corresponding metal salts are shown in scheme 3. **HL** (**1**) binds with nickel and cobalt ions with a 2 : 1 M ratio forming octahedral geometry around the metal. However, physicochemical analyses reveal that the Cu(II) complex has five-coordinate binuclear square pyramidal geometry around Cu(II). A new FT-IR band around 1297 cm^{-1} was observed for coordinated nitrate in **3**. The Pd(II) complex shows distorted square planar geometry. Molar conductivity studies reveal that the metal complexes are non-electrolytes. The reaction scheme is shown in scheme 3.



Scheme 3. Synthesis of metal complexes.

3.2. $^1\text{H-NMR}$ spectra of **HL** (**1**) and $[\text{PdLCI}]\cdot 0.5(\text{CH}_2\text{Cl}_2)$ (**5**)

The $^1\text{H-NMR}$ (300 MHz) spectra of **HL** and **5** were recorded in CDCl_3 . A singlet for phenolic OH is at 15.317 ppm for **HL**, shifted downfield due to the presence of phenol–amine hydrogen bonding. A singlet for benzilidimine proton is at 9.22 ppm. The aromatic (Ar–H) and benzylic (CH_2) protons are a multiplet and singlet at 7.1–8.09 and 4.1 ppm, respectively.

In the spectrum of Pd(II) complex, the OH proton disappears, signifying the deprotonation upon complexation. Peaks at 8.95, 7.12–7.88, and 4.45 ppm appeared for $\text{CH}=\text{N}$, aromatic protons, and CH_2 protons, respectively. The methylene proton appeared as two separate doublets having germinal-coupling.

3.3. Magnetic measurements

The magnetic moment (μ_{eff}) for Ni(II) complex is 2.80 BM, near to the expected value of d^8 octahedral symmetry. The binuclear Cu(II) complex possesses magnetic moment value of 1.62 BM, smaller than spin-only value [54]; the Co(II) complex shows magnetic moment of 4.81 BM for high-spin octahedral symmetry, and the Pd(II) complex is diamagnetic.

3.4. Electronic spectra

Electronic spectra of the ligand at 10^{-4} M and complexes at 2×10^{-4} M in DMF are shown in figure 1. Electronic spectra of the ligand and its complexes are also taken in higher concentrations (10^{-3} M) for the region 500–800 nm, shown as insets in figure 1. The electronic spectrum of ligand shows peaks at 267, 319, 392, and 466 nm which may be assigned to

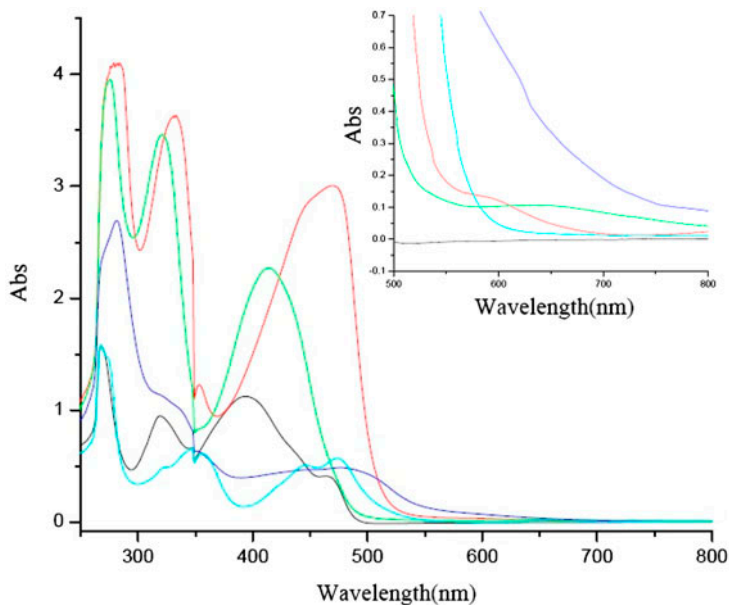


Figure 1. Electronic spectra of **1** (10^{-4} M) (–), **2** (2×10^{-4} M) (–), **3** (2×10^{-4} M) (–), **4** (2×10^{-4} M) (–), and **5** (2×10^{-4} M) (–) in DMF.

Table 2. Electronic spectral data of **1**–**5**.

Compound	λ (nm)	ϵ_{\max} ($M^{-1} \text{ cm}^{-1}$)
Ligand, 1	267	15,600
	319	9490
	392	11,250
	466	4020
Ni(II) complex, 2	281	20,450
	331	18,050
	496	15,000
Cu(II) complex, 3	601	160
	275	19,650
	320	17,250
	413	11,300
Co(II) complex, 4	652	120
	281	13,400
	322	5625
	485	2410
Pd(II) complex, 5	624	500
	268	7965
	347	3000
	356	3100
	444	2575
	472	2500

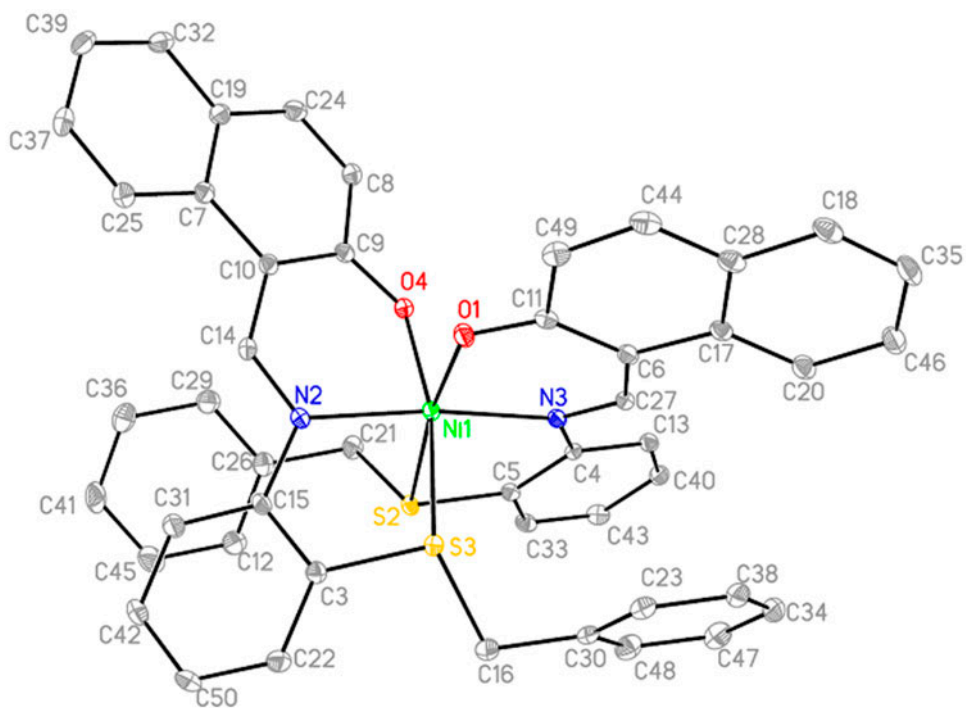


Figure 3. Molecular structure of 2 with 50% probability ellipsoids.

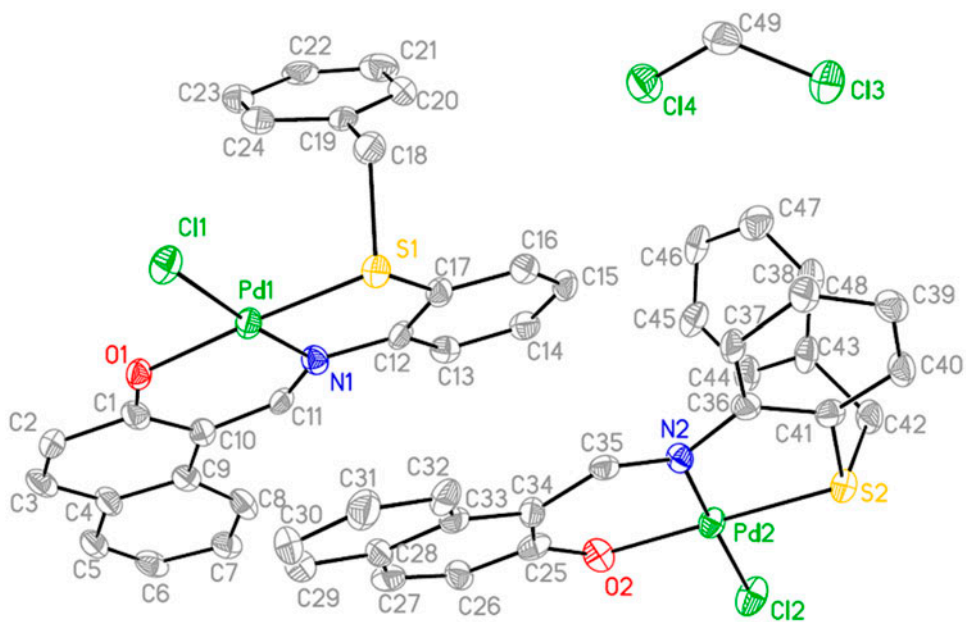


Figure 4. Molecular structure of 5 with 50% probability ellipsoids.

Table 3. Selected bond lengths (Å) and angles (°) for **1**.

Bond lengths	(Å)	Bond angles	(°)
S(1)–C(1)	1.777(5)	C(1)–S(1)–C(18)	102.4(2)
S(1)–C(18)	1.821(5)	C(9)–O(1)–H(1A)	119(3)
O(1)–C(9)	1.343(6)	C(7)–N(1)–C(6)	122.7(4)
O(1)–H(1A)	1.020(6)	N(1)–C(6)–C(1)	115.8(4)
N(1)–C(7)	1.295(6)	N(1)–C(7)–C(8)	122.2(4)
N(1)–C(6)	1.415(6)	O(1)–C(9)–C(8)	122.1(5)
C(7)–C(8)	1.446(7)	C(19)–C(18)–S(1)	108.0(4)
C(7)–H(7)	0.930(4)		

Compound **2** crystallizes in the triclinic space group P-1 containing one molecule in the asymmetric unit. The crystal shows lower R, wR, and bond length e.s.d values compared to the reported one [55], indicating better crystallographic data [56]. Two deprotonated ligand units coordinate through N₂S₂O₂-donors forming octahedral Ni(II) complex. The C–N, C–S, and C–O bond lengths in Ni(II) complex are shifted compared to the free ligand. The imine bond N(3)–C(27) increases to 1.308(3) Å from 1.295(6) Å and S(2)–C(21) increases to 1.839(2) Å from 1.821(5) Å due to the donation of electron cloud of N and S to nickel. However, the O(1)–C(11) bond decreases to 1.287(3) Å from 1.343(6) Å due to the delocalization of negative charge of deprotonated oxygen to the ligand, acquiring partial double bond character. The two deprotonated oxygens of two ligands bonded to Ni(II) are *cis* to each other and two sulfurs also *cis*. These four donors are the basal plane and two nitrogens are axial at an angle N(3)–Ni(1)–N(2), 173.43(7)°. The bite angles O(1)–Ni(1)–O(4), O(4)–Ni(1)–S(2), O(1)–Ni(1)–S(3), and S(2)–Ni(1)–S(3) are 93.03(6)°, 92.54(4)°, 84.66(4)°, and 90.910(19)°, respectively. All the bite angles deviate from 90°, indicating that the Ni(II) complex has distorted octahedral geometry. All the important bond lengths and angles of **2** are given in table 4.

Complex **5** crystallizes in the monoclinic space group P2(1)/c containing two molecules in the asymmetric unit. One DCM molecule is also observed in the asymmetric unit of the crystal lattice. Important bond lengths and angles of **5** are given in table 5. The Pd–S and Pd–O bond lengths show regular Pd–S and Pd–O bond lengths [57]. Pd(II) coordinates with O, N, and S of the ligand and one Cl[−] to fulfill the square planar geometry. The bite angles O(1)–Pd(1)–Cl(1), S(1)–Pd(1)–Cl(1), O(2)–Pd(2)–N(2), and N(2)–Pd(2)–S(2) are 89.1(2)°,

Table 4. Selected bond lengths (Å) and angles (°) for **2**.

Bond lengths	(Å)	Bond angles	(°)
Ni–O(1)	1.9979(15)	O(1)–Ni(1)–O(4)	93.03(6)
Ni–O(4)	2.0074(14)	O(1)–Ni(1)–N(3)	90.69(6)
Ni–N(3)	2.0235(17)	O(4)–Ni(1)–N(3)	96.32(6)
Ni–N(2)	2.0281(17)	O(1)–Ni(1)–N(2)	93.83(7)
Ni–S(2)	2.4390(6)	O(4)–Ni(1)–N(2)	88.20(6)
Ni–S(3)	2.5267(6)	N(3)–Ni(1)–N(2)	173.43(7)
O(1)–C(11)	1.287(3)	O(1)–Ni(1)–S(2)	172.70(5)
O(4)–C(9)	1.288(3)	O(4)–Ni(1)–S(2)	92.54(4)
N(2)–C(14)	1.304(3)	N(3)–Ni(1)–S(2)	84.00(5)
N(2)–C(15)	1.423(2)	N(2)–Ni(1)–S(2)	91.06(5)
N(3)–C(27)	1.308(3)	O(1)–Ni(1)–S(3)	84.66(4)
N(3)–C(4)	1.421(3)	O(4)–Ni(1)–S(3)	167.32(4)
S(2)–C(5)	1.778(2)	N(3)–Ni(1)–S(3)	96.17(5)
S(2)–C(21)	1.839(2)	N(2)–Ni(1)–S(3)	79.53(5)
S(3)–C(3)	1.775(2)	S(2)–Ni(1)–S(3)	90.910(19)
S(3)–C(16)	1.833(2)		

Table 5. Selected bond lengths (Å) and angles (°) for **5**.

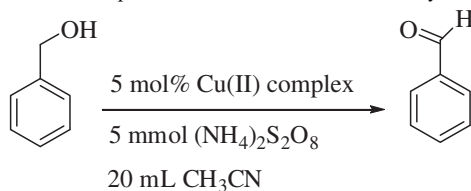
Bond lengths	(Å)	Bond angles	(°)
Pd(1)–O(1)	2.004(8)	O(1)–Pd(1)–N(1)	92.9(3)
Pd(1)–N(1)	2.010(9)	O(1)–Pd(1)–S(1)	176.7(2)
Pd(1)–S(1)	2.231(3)	N(1)–Pd(1)–S(1)	87.6(3)
Pd(1)–Cl(1)	2.322(3)	O(1)–Pd(1)–Cl(1)	89.1(2)
Pd(2)–O(2)	1.978(9)	N(1)–Pd(1)–Cl(1)	175.8(3)
Pd(2)–N(2)	2.004(8)	S(1)–Pd(1)–Cl(1)	90.60(10)
Pd(2)–S(2)	2.232(3)	O(2)–Pd(2)–N(2)	93.0(4)
Pd(2)–Cl(2)	2.330(3)	O(2)–Pd(2)–S(2)	179.5(3)
S(2)–C(41)	1.793(11)	N(2)–Pd(2)–S(2)	87.0(3)
S(2)–C(42)	1.854(13)	O(2)–Pd(2)–Cl(2)	89.0(3)
S(1)–C(17)	1.779(11)	N(2)–Pd(2)–Cl(2)	176.3(3)
S(1)–C(18)	1.854(12)	S(2)–Pd(2)–Cl(2)	90.92(11)
Cl(4)–C(49)	1.730(15)		
Cl(3)–C(49)	1.788(16)		
O(1)–C(1)	1.269(15)		
O(2)–C(25)	1.321(16)		
N(2)–C(35)	1.303(15)		
N(2)–C(36)	1.428(15)		
N(1)–C(11)	1.279(16)		
N(1)–C(12)	1.436(14)		

90.60(10)°, 93.0(4)°, and 87.0(3)°, respectively; angles N(1)–Pd(1)–Cl(1) and O(2)–Pd(2)–S(2) at 175.8(3)° and 179.5(3)° confirm slightly distorted square planar geometry.

3.6. Cu(II) complex catalyzed aerobic oxidation of alcohol to aldehyde

The reaction conditions were optimized by performing a series of experiments with different solvents, oxidants, catalysts, and reaction time. The optimized reaction conditions for benzyl alcohol and the results are shown in table 6; 5 mol% Cu(II) complex as catalyst and 5 mmol ammonium persulfate as oxidant were optimum concentrations for the conversion

Table 6. Optimized reaction condition for benzyl alcohol to benzaldehyde at room temperature.

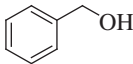
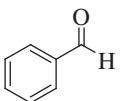
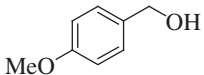
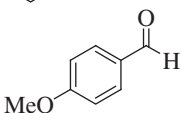
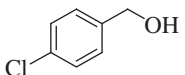
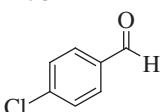
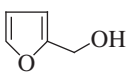
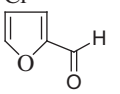
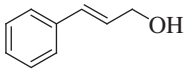
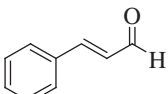
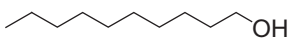
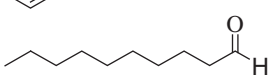
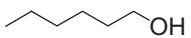
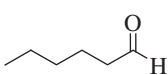
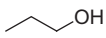
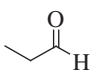
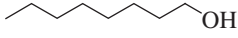
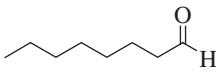


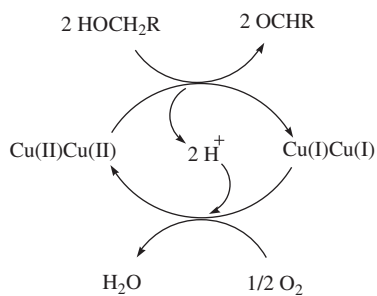
Entry	Catalyst	Oxidant	Solvent	Time	Conversion%	Yield
1	None	(NH ₄) ₂ S ₂ O ₈	CH ₃ CN	24 h	0	0
2	CuCl ₂	(NH ₄) ₂ S ₂ O ₈	CH ₃ CN	4 h	56	50
3	Cu(II) complex	(NH₄)₂S₂O₈	CH₃CN	2 min	100	96
4	Cu(II) complex	H ₂ O ₂	CH ₃ CN	2 h	80	71
5	Cu(II) complex	(NH ₄) ₂ S ₂ O ₈	CH ₂ Cl ₂	15 min	82	74
6	Cu(II) complex	(NH ₄) ₂ S ₂ O ₈	DMF	30 min	40	29
7	Cu(II) complex	(NH ₄) ₂ S ₂ O ₈	DMSO	30 min	42	32
8	Cu(II) complex	(NH ₄) ₂ S ₂ O ₈	THF	30 min	51	41

The significance of bold values shows the optimized reaction conditions for benzyl alcohol.

Table 7. Oxidation of alcohol to aldehyde catalyzed by Cu(II) complex in $\text{CH}_3\text{CN}-(\text{NH}_4)_2\text{S}_2\text{O}_8$ system.

$$\text{R}-\text{CH}_2\text{OH} \xrightarrow[\substack{5 \text{ mmol } (\text{NH}_4)_2\text{S}_2\text{O}_8 \\ 20 \text{ mL } \text{CH}_3\text{CN}}]{5 \text{ mol\% Cu(II) complex}} \text{R}-\overset{\text{O}}{\parallel}{\text{C}}-\text{H}$$

Entry	Substrate	Product	Time (min)	Yield (%)
1			2	96
2			3	92
3			5	86
4			4	86
5			6	92
6			4	92
7			4	91
8			3	89
9			4	93



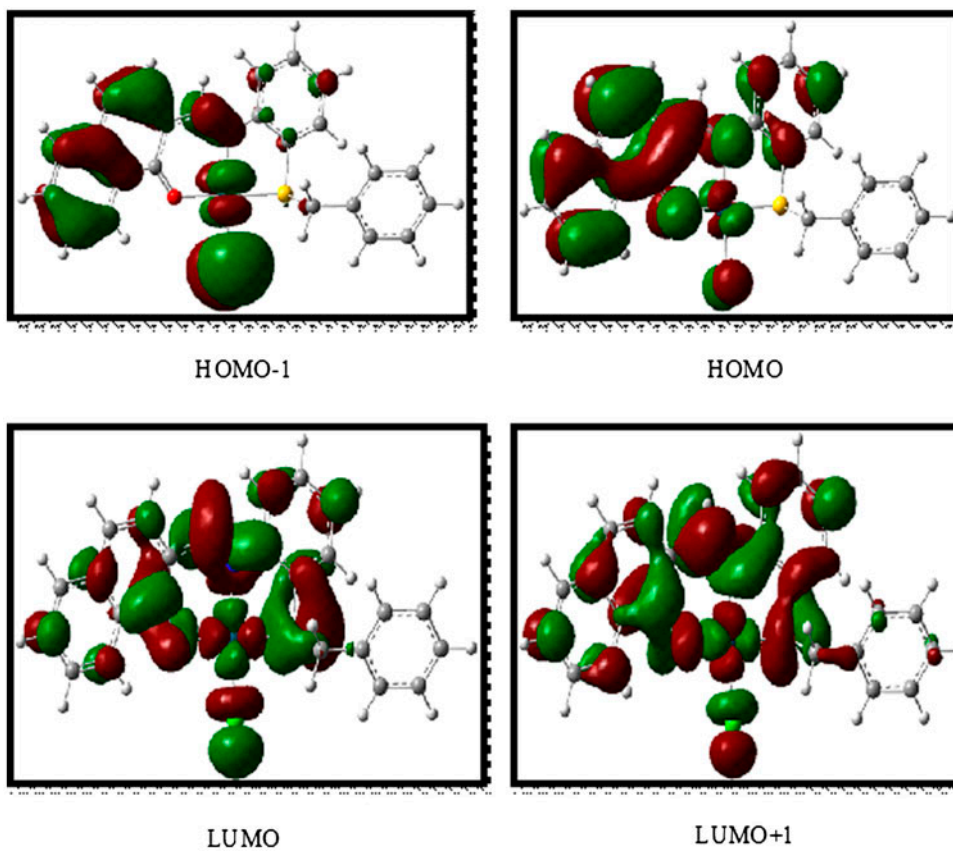
Scheme 4. Probable mechanism for the oxidation of alcohol to aldehyde.

Table 8. The experimental and calculated bond lengths (Å) and angles (°) for **5**.

Bond lengths	Expt	Calcd	Bond angles	Expt	Calcd
Pd(1)–O(1)	2.004(8)	2.028	O(1)–Pd(1)–N(1)	92.9(3)	93.69
Pd(1)–N(1)	2.010(9)	2.043	O(1)–Pd(1)–S(1)	176.7(2)	178.73
Pd(1)–S(1)	2.231(3)	2.303	N(1)–Pd(1)–S(1)	87.6(3)	86.64
Pd(1)–Cl(1)	2.322(3)	2.358	O(1)–Pd(1)–Cl(1)	89.1(2)	90.20
S(1)–C(17)	1.779(11)	1.797	N(1)–Pd(1)–Cl(1)	175.8(3)	175.77
S(1)–C(18)	1.854(12)	1.883	S(1)–Pd(1)–Cl(1)	90.60(10)	89.51
O(1)–C(1)	1.269(15)	1.283			
N(1)–C(11)	1.279(16)	1.321			
N(1)–C(12)	1.436(14)	1.420			

of 4 mmol benzyl alcohol to benzaldehyde in 20 mL acetonitrile. The oxidation reaction was performed for different alcohols as shown in table 7. **3** exhibits very good catalytic activity with high yield at room temperature.

We proposed the mechanism of binuclear Cu(II) complex catalyzed oxidation of primary alcohol to aldehyde. Cu(II)Cu(II) binuclear complex undergoes reduction to intermediate

Figure 5. Contour plots of HOMOs and LUMOs of **5**.

Cu(I)Cu(I) form without breaking the oxobridge [58] in CH₃CN and oxidizes alcohol to aldehyde. Here, (NH₄)₂S₂O₈ enhances the formation of molecular oxygen in the system and helps the conversion of Cu(I)Cu(I) to Cu(II)Cu(II) by releasing water as by-product to complete the catalytic cycle [59–63]. The reaction takes place by two electron transfers from alcohol to binuclear Cu(II)Cu(II) complex. Intermediate Cu(I)Cu(I) is stabilized by CH₃CN, hence the reaction is efficient. The probable mechanism for oxidation of alcohol is given in scheme 4.

3.7. DFT calculation

The optimized geometry of **5** was performed by DFT/B3LYP method. The calculated bond distances and angles are included in table 8. The calculated structural parameters are in agreement with the experimentally observed data. The Pd–S bond of the complex shows maximum deviation of 0.072 Å compared with other metal–atom bonds. The contour plots of HOMO – 1, HOMO, LUMO, and LUMO + 1 of the complex are shown in figure 5.

4. Conclusion

We have synthesized a tridentate ONS donor and four complexes and characterized by spectral and single-crystal X-ray diffraction analysis. Complexes **2** and **4** have the 2 : 1 ratio of tridentate ligand : metal ion and **3** and **5** have the 1 : 1 ratio of tridentate ligand : metal ion. The geometry of the Ni(II) complex is slightly distorted octahedral and Pd(II) complex is slightly distorted square planar. We have developed a catalytic system using the Cu(II) complex and (NH₄)₂S₂O₈ for selective oxidation of alcohol to aldehyde in acetonitrile. The system is attractive due to simple procedure, environmentally benign, high yield within shorter reaction at room temperature. The DFT study of the Pd(II) complex **5** using B3LYP method show quite good agreement with the data obtained from single-crystal X-ray diffraction studies.

Supplementary material

CCDC 997116, 997117, and 997118 contains the supplementary crystallographic data for the ligand, the Ni(II) complex, and the Pd(II) complex, respectively. These data can be obtained free of charge via <http://www.ccdc.cam.ac.uk/conts/retrieving.html> or from the Cambridge Crystallographic Data Center, 12 Union Road, Cambridge CB2 1EZ, UK; Fax: (+44) 1223-336-033; or E-mail: deposit@ccdc.cam.ac.uk.

Acknowledgments

The authors gratefully acknowledge Indian Association for the Cultivation of Science, Kolkata, for the Gaussian 09 program package, Tezpur University, Tezpur and IIT Bombay, Mumbai, for spectral and analytical data. Also thanks to Director of NIT, Silchar, for financial assistance (K.S, N.D, and M.K).

Disclosure statement

No potential conflict of interest was reported by the authors.

Supplemental data

Supplemental data for this article can be accessed here [<http://dx.doi.org/10.1080/00958972.2015.1075241>].

References

- [1] Z.L. You, H.L. Zhu. *Z. Anorg. Allg. Chem.*, **630**, 2754 (2004).
- [2] K.P. Balasubramanian, K. Parameswari, V. Chinnusamy, R. Prabhakaran, K. Natarajan. *Spectrochim. Acta, Part A*, **65**, 678 (2006).
- [3] K.S. Murray, A.M. van den Bergen, B.O. West. *Aust. J. Chem.*, **31**, 203 (1978).
- [4] H. Doine, F.F. Stephens, R.D. Cannon. *Bull. Chem. Soc. Jpn.*, **58**, 1327 (1985).
- [5] K. Nakajima, Y. Ando, H. Mano, M. Kojima. *Inorg. Chim. Acta*, **274**, 184 (1998).
- [6] B.D. Clercq, F. Verpoort. *Macromolecules*, **35**, 8943 (2002).
- [7] T. Opstal, F. Verpoort. *Synlett*, **6**, 0935 (2002).
- [8] T. Opstal, F. Verpoort. *Angew. Chem. Int. Ed.*, **42**, 2876 (2003).
- [9] S.N. Pal, S. Pal. *Inorg. Chem.*, **40**, 4807 (2001).
- [10] B.D. Clercq, F. Verpoort. *Adv. Synth. Catal.*, **344**, 639 (2002).
- [11] B.D. Clercq, F. Lefebvre, F. Verpoort. *Appl. Catal. A*, **247**, 345 (2003).
- [12] A. Patra, S. Sarkar, M.G.B. Drew, E. Zangrando, P. Chattopadhyay. *Polyhedron*, **28**, 1261 (2009).
- [13] S.A. Patil, V.H. Naik, A.D. Kulkarni, P.S. Badami. *Spectrochim. Acta, Part A*, **75**, 347 (2010).
- [14] A.K. Nandi, S. Chaudhuri, S.K. Mazumdar, S. Ghosh. *J. Chem. Soc., Perkin Trans. 2*, **11**, 1729 (1984).
- [15] M.A. Ali, D.A. Chowdhury-I, M.N. Uddin. *Polyhedron*, **3**, 595 (1984).
- [16] J.P. Scovill, D.L. Klayman, C.F. Franchino. *J. Med. Chem.*, **25**, 1261 (1982).
- [17] N.K. Singh, S.B. Singh. *Ind. J. Chem., Sect. A*, **40A**, 1070 (2001).
- [18] R.K. Agarwal, L. Singh, D.K. Sharma. *Bioinorg. Chem. Appl.*, **2006**, 1 (2006).
- [19] M.E. Hossain, M.N. Alam, J. Begum, M.A. Ali, M. Nazimuddin, F.E. Smith, R.C. Hynes. *Inorg. Chim. Acta*, **249**, 207 (1996).
- [20] P. Bindu, M.R.P. Kurup, T.R. Satyakeerty. *Polyhedron*, **18**, 321 (1998).
- [21] A.K. Pramanik, M.S. Jana, T.K. Mondal. *J. Coord. Chem.*, **66**, 4067 (2013).
- [22] M. Kalita, P. Gogoi, P. Barman, B. Sarma. *J. Coord. Chem.*, **67**, 2445 (2014).
- [23] P. Gogoi, S. Hazarika, M.J. Sarma, K. Sarma, P. Barman. *Tetrahedron*, **70**, 7484 (2014).
- [24] D. Banerjee, U. Ray, S. Jasimuddin, J.C. Liou, T.H. Lu, C. Sinha. *Polyhedron*, **25**, 1299 (2006).
- [25] R. Balamurugan, M. Palaniandavar, M.A. Halcrow. *Polyhedron*, **27**, 1077 (2006).
- [26] B. Turner, S. Swavey. *Inorg. Chem. Commun.*, **10**, 209 (2007).
- [27] M.M. Tamizh, R. Karvembu. *Inorg. Chem. Commun.*, **25**, 30 (2012).
- [28] J. Hurtado, M. Portaluppi, R. Quijada, R. Rojas, M. Valderrama. *J. Coord. Chem.*, **62**, 2772 (2009).
- [29] D.Y. Ma, L.X. Zhang, X.Y. Rao, T.L. Wu, D.H. Li, X.Q. Xie. *J. Coord. Chem.*, **66**, 1486 (2013).
- [30] K. Karami. *J. Coord. Chem.*, **63**, 3688 (2010).
- [31] K.C. Gupta, A.K. Sutar. *Coord. Chem. Rev.*, **252**, 1420 (2008).
- [32] S. Ray, S. Jana, A. Jana, S. Konar, K. Das, S. Chatterjee, R.J. Butcher, S.K. Kar. *Polyhedron*, **46**, 74 (2012).
- [33] I.E. Marko, A. Gautier, R. Dumeunier. *Angew. Chem. Int. Ed.*, **43**, 1588 (2004).
- [34] P. Gamez, I.W.C.E. Arends, J. Reedijk, R.A. Sheldon. *Chem. Commun.*, **19**, 2414 (2003).
- [35] P. Belanzoni, C. Michel, E.J. Baerends. *Inorg. Chem.*, **50**, 11896 (2011).
- [36] Y. Zhu, B. Zhao, Y. Shi. *Org. Lett.*, **15**, 992 (2013).
- [37] J.M. Hoover, S.S. Stahl. *J. Am. Chem. Soc.*, **133**, 16901 (2011).
- [38] N. Tyagi, R. Kumar, K. Mahiya, P. Mathur. *J. Coord. Chem.*, **66**, 3335 (2013).
- [39] Z. Nadealian, V. Mirkhani, B. Yadollahi, M. Moghadam, S. Tangestaninejad, I.M. Baltork. *J. Coord. Chem.*, **66**, 1264 (2013).
- [40] X.F. Yin, H. Lin, A.Q. Jia, Q. Chen, Q.F. Zhang. *J. Coord. Chem.*, **66**, 3229 (2013).
- [41] C.K. Modi, P.M. Trivedi. *J. Coord. Chem.*, **67**, 3678 (2014).
- [42] R. Benramdane, F. Benghanem, A. Ourari, S. Keraghel, G. Bouet. *J. Coord. Chem.*, **68**, 560 (2015).
- [43] S. Velusamy, A. Srinivasan, T. Punniyamurthy. *Tetrahedron Lett.*, **47**, 923 (2006).
- [44] P. Gamez, I.W.C.E. Arends, R.A. Sheldon, J. Reedijk. *Adv. Synth. Catal.*, **346**, 805 (2004).
- [45] P. Belanzoni, C. Michel, E.J. Baerends. *Inorg. Chem.*, **50**, 11896 (2011).

- [46] A. Pui. *Synth. React. Inorg. Met.-Org. Nano-Met. Chem.*, **36**, 523 (2006).
- [47] D.A. Rockcliffe, A.E. Martell. *J. Mol. Catal. A: Chem.*, **106**, 211 (1996).
- [48] Q.X. Shi, R.W. Lu, Z.X. Zhang, D.F. Zhao. *Chin. Chem. Lett.*, **17**, 1045 (2006).
- [49] D.D. Perrin, W.L.F. Armarego. *Purification of Laboratory Chemicals*, 3rd Edn, Pergamon, New York (1988).
- [50] G.M. Sheldrick. *Acta Crystallogr. A*, **64**, 112 (2008).
- [51] G.M. Sheldrick. *SHELXS-97 and SHELXL-97, Fortran Programs for Crystal Structure Solution and Refinement*. University of Gottingen, Gottingen (1997).
- [52] SMART, SAINT and SADABS, Bruker AXS Inc., Madison, WI (2007).
- [53] M.J. Frisch, G.W. Trucks, H.B. Schlegel, G.E. Scuseria, M.A. Robb, J.R. Cheeseman, G. Scalmani, V. Barone, B. Mennucci, G.A. Petersson, *Gaussian 09, Revision C.01*, Gaussian, Inc., Wallingford, CT (2010).
- [54] P. Kamatchi, S. Selvaraj, M. Kandaswamy. *Polyhedron*, **24**, 900 (2005).
- [55] P. Pattanayak, J.L. Pratihar, D. Patra, P. Brandao, V. Felix. *Inorg. Chim. Acta*, **418**, 171 (2014).
- [56] P.G. Jones. *Chem. Soc. Rev.*, **13**, 157 (1984).
- [57] S. Acharya, A. Kejriwal, A.N. Biswas, P. Das, D.N. Neogi, P. Bandyopadhyay. *Polyhedron*, **38**, 50 (2012).
- [58] L.R. Martins, E.T. Souza, T.L. Fernandez, B. de Souza, S. Rachinski, C.B. Pinheiro, R.B. Faria, A. Casellato, S.P. Machado, A.S. Mangrich, M. Scarpellini. *Braz. Chem. Soc.*, **21**, 1218 (2010).
- [59] E.A. Lewis, W.B. Tolman. *Chem. Rev.*, **104**, 1047 (2004).
- [60] J.P. Klinman. *Chem. Rev.*, **96**, 2541 (1996).
- [61] R.H. Holm, P. Kennepohl, E.I. Solomon. *Chem. Rev.*, **96**, 2239 (1996).
- [62] K. Asami, K. Tsukidate, S. Iwatsuki, F. Tani, S. Karasawa, L. Chiang, T. Storr, F. Thomas, Y. Shimazaki. *Inorg. Chem.*, **51**, 12450 (2012).
- [63] D. Das, Y.M. Lee, K. Ohkubo, W. Nam, K.D. Karlin, S. Fukuzumi. *J. Am. Chem. Soc.*, **135**, 2825 (2013).